



# The use of a SQUID for quantitative magnetic field measurements in the nanoTesla region for eddy current NDE

N. Poulakis

Electrical Engineering Department, Technological Educational Institute of West Macedonia, Greece  
[poulakis@kozani.teiko.gr](mailto:poulakis@kozani.teiko.gr)

T. Theodoulidis

Department of Engineering and Management of Energy Resources, University of West Macedonia, Greece  
[theodoul@uowm.gr](mailto:theodoul@uowm.gr)

*Abstract - In this paper the use of a HTS SQUID magnetometer for quantitative measurements in eddy current NDE is presented. The SQUID is used in absolute rather than in gradiometric mode and the magnetic field measurements are directly compared to theoretical results. The measurements are taken in an ambient noise environment and the excitation has the form of a double-rectangle Printed Circuit Board coil. The configurations examined involve the coil in air and above Aluminum plates with or without defects in the form of long through-thickness slots. The agreement between experimental and theoretical results is very good showing that model-based calculations and optimizations of SQUID magnetometers are feasible.*

**Keywords:** SQUID, eddy current testing, magnetic field measurement, PCB coil.

## 1 Introduction

There are two general methods to measure the eddy current (EC) response, i.e., the magnitude and phase of the magnetic field (MF) generated by eddy currents in a conductive testpiece during a nondestructive inspection: (i) the indirect method, using coils and measuring their complex impedance (in absolute, differential or driver-pickup mode) and (ii) the direct method, using coil excitation and measuring the resulting MF with sensors like Hall probes, GMR probes and SQUIDs.

Eddy current testing traditionally relies on the former, i.e. the detection of impedance changes of a pickup coil while this is moved across the inspected specimen. However, in order to detect deep flaws in conductive materials, low excitation frequencies are required to achieve a sufficient penetration depth. Since the sensitivity of normal pickup coils is proportional to the excitation frequency, standard eddy current techniques are insufficient for deep subsurface flaw detection. In such cases it is advantageous to measure directly the magnetic field rather than its time rate of change (coil impedance change). Among the available MF sensors, the SQUID is by far the most sensitive, thus making it ideal for the measurement of weak magnetic field perturbations resulting from deep lying defects [1-3]. Although it requires cooling of the device to achieve superconducting conditions, it has nevertheless gained considerable attention during the last years and much applied research is performed with the ultimate goal of its commercialization in the field of NDE.

A common characteristic of all MF measurement techniques is that magnetometers are used in differential (comparative) mode, i.e., they measure MF changes relative to an offset value. This is mainly due to lack of knowledge of the transfer function (output voltage as a function of magnetic field intensity) which is an intrinsic problem of the MF sensors used. Calibration of the output voltage of MF sensors needs standard



prototype MF set-ups of known intensity which are neither easy to create nor practical. From this point of view, SQUID sensors have the unique characteristic of their output voltage to be intrinsically related to a physical constant, the quantum of magnetic flux,  $\Phi_0 = h/2e = 2.07 \times 10^{-15}$  Wb. Other SQUID characteristics are the ultra low magnetic field noise  $< 100$  fT/ $\sqrt{\text{Hz}}$  even at low frequencies of 1 Hz, high spatial resolution, high linearity and operating field up to 1 mT. SQUIDs are used either as magnetometers, in which case a lock-in amplifier is utilized to reject the environmental noise from the single sensor and enable measurement at a specific frequency, or as double electronic gradiometers where the difference of the signals from two nearby sensors is utilized (differential mode). The problem with the latter case is that the signal interpretation is difficult and not directly comparable to theory.

In this work, a SQUID magnetometer is used in the absolute mode with the aim to compare experimental MF measurements directly to theoretical models. Previous work has been done regarding the use of theory for optimizing the SQUID system measurement parameters such as sensitivity to flaws, position of coil and sensor, coil geometry, driving current amplitude and form and signal interpretation. This involved empirical models or the use of time consuming FEM [4], simplifying exciter geometries in the form of circular filamentary loops [5-6], modeling of double-D filamentary coils [7] and also numerical methods for simulating defects in the inspected conductive testpiece [8]. The inherent complexity in modeling 3D electromagnetic field problems has also led researchers in adopting simplified models like infinite current sheets and to apply these simplified models for approximating the more complicated 3D configurations [9].

In the next paragraphs we briefly describe the measurement system and then present experimental and theoretical results for an excitation in the form of a double-rectangle PCB coil. Some preliminary results with the same SQUID system were presented in [10] and [11] for excitations in the form of precision wound circular coils.

## 2 SQUID measurement system

A HTS SQUID system was integrated to a scanning unit and thus a complete measuring unit for experimental investigations was developed, a detailed description can be found in [10]. The SQUID sensor is made out of high temperature superconducting material (HTS) mounted in a simple carbon reinforced plastic dewar vessel and cooled with liquid nitrogen (LN<sub>2</sub>). The SQUID sensor as well as its electronic control modules (Programmable Feedback Loop and PC Interface Unit) has been constructed by STAR Cryoelectronics [12]. The output voltage is directed to a lock-in amplifier. As reference signal to the lock-in amplifier, the TTL SYNC output of a high quality signal generator (SRS DS340) was used. The generator's voltage output was used for the sine excitation of the coil. The phase shift between output voltage and current in the coil was corrected for each frequency within 0.1° accuracy with the coil in air. In this way, the lock-in amplifier's reference was always in phase to the coil excitation current and directly comparable to the theoretical calculations. The in-phase and quadrature components of the SQUID voltage output along with the coil rms current (measured with 4 1/2 digits precision) are recorded and multiplied by the SQUID transfer function  $1.71\Phi_0/V \times 8.78\text{nT}/\Phi_0 = 15.01\text{nT}/V$  and the final results are presented in nT per mA of excitation current. Calculation of the transfer function value from the standard calibration procedure was described also in [10].

When measuring the magnetic field in eddy current testing there are two magnetic fields present that are superposed. The first is the incident magnetic field from the excitation  $B_{\text{excitation}}$  and the second is the reaction field associated to the induced eddy currents in the inspected specimen. The eddy current distribution in a metal (and its associated magnetic field  $B_{\text{eddy}}$ ) is disturbed when the eddy currents are induced in a region containing a flaw. The presence of a flaw in metal specimens can be detected by measuring the change in  $B_{\text{eddy}}$  as the sensor is moved from an unflawed region to one containing a flaw. However, the incident magnetic field  $B_{\text{excitation}}$  is relatively large and appropriate means for eliminating it

should be applied. SQUID-based eddy current experiments are usually carried out using a “double-D” excitation coil, consisting of windings in the shape of two Ds with their straight sections carrying current in the same direction and parallel to each other. The normal component of the magnetic field is zero on the central axis of the double-D exciter. A non-zero magnetic field is sensed whenever there is some sort of asymmetry below the measurement system as in the case of the SQUID passing over a region with a flaw. The use of the double-D coil reduces the background signals (noise) and hence enhances the ease with which small and/or deep flaws may be detected. Hence the dynamic range of measurement is extended. The winding, however, of a totally symmetric double-D coil is difficult and this is the reason for our choice of a PCB coil that can have exact dimensions and thus be very well characterized. Moreover instead of a double-D shape and in order to facilitate the coil modeling, a double-rectangle was used, as shown in Fig.1.

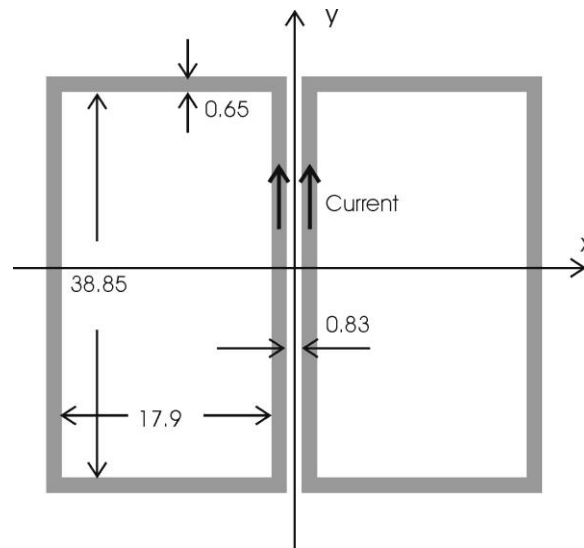


Fig.1 Top view of the double-rectangle PCB coil that was used as excitation. The copper layer thickness is  $30\mu\text{m}$ .

An additional reason for using a double-coil excitation was the excessive output signal from the SQUID when coil arrangements in the form of usual circular coils were used. Even moderate currents of the order of  $0.1\text{mA}$  could saturate the sensitive SQUID sensor, thus necessitating the application of even lower amplitude excitation currents. With the double-rectangle coil we can increase the excitation current at will and in this way we can amplify weak signals from subsurface flaws.

Incidentally, there is a lot of interest lately in using rectangular spiral coils for eddy current NDE, owing to their high sensitivity to cracks because of the small effective lift-off, straightforward manufacture using PCB technology, easy and unobtrusive permanent attachment to the part being inspected and the prospect of using flexible PCB coils to allow the coil to conform to a curved surface [14-15].

### 3 Results and Discussion

In this section we present experiments and compare to theoretical results for the double-rectangle coil of Fig.1. Early experimental measurements and comparison to theoretical results were done for a circular coil in air (magnetic field as a function of distance), a circular coil above a conductive plate (frequency scan measurements) and a circular coil moving across a long slot in a thin plate [11].

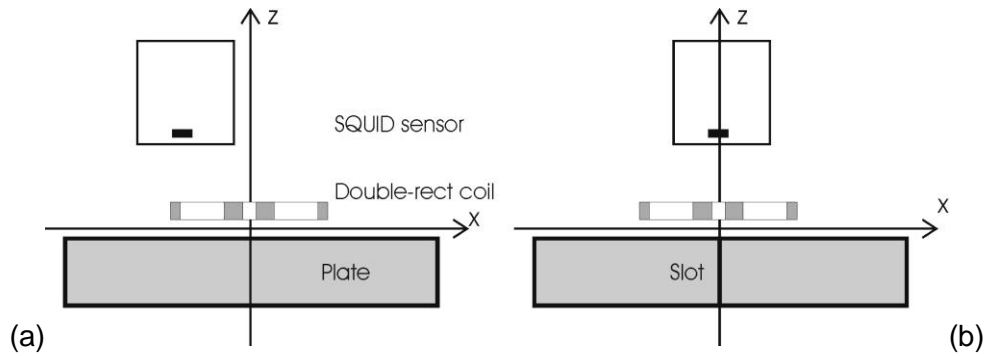


Fig.2 Magnetic field measurement using a SQUID sensor (a) Excitation coil in air or above plate without defect, only the SQUID sensor is moved (b) Coil above plate with defect, SQUID sensor and excitation coil are moved together.

### 3.1 Isolated coil

Measurements of the magnetic field with the coil in air away from any conductive media, were taken first. In this case the SQUID was moved above the coil in the  $x$ -direction at  $y=0$  (passing above the coil center) at a height of 28.9mm. The magnetic field is in phase with the excitation current and thus only its real part is measured. Fig.3a shows the variation of  $B_z$  with respect to the distance along the  $x$ -axis. As expected, the field has an odd symmetry around  $x=0$ , at which value it vanishes. The theoretical results were derived by using an existing model for rectangular coils [13] and their agreement with experimental results is excellent. More theoretical results were produced, see Fig.3b, and another feature observed was the fact that the decrease of the magnetic field maximum with vertical distance was a function of  $z^{-2.7}$ , which is close to  $z^{-2.5}$  the known theoretical behavior for the magnetic dipole.

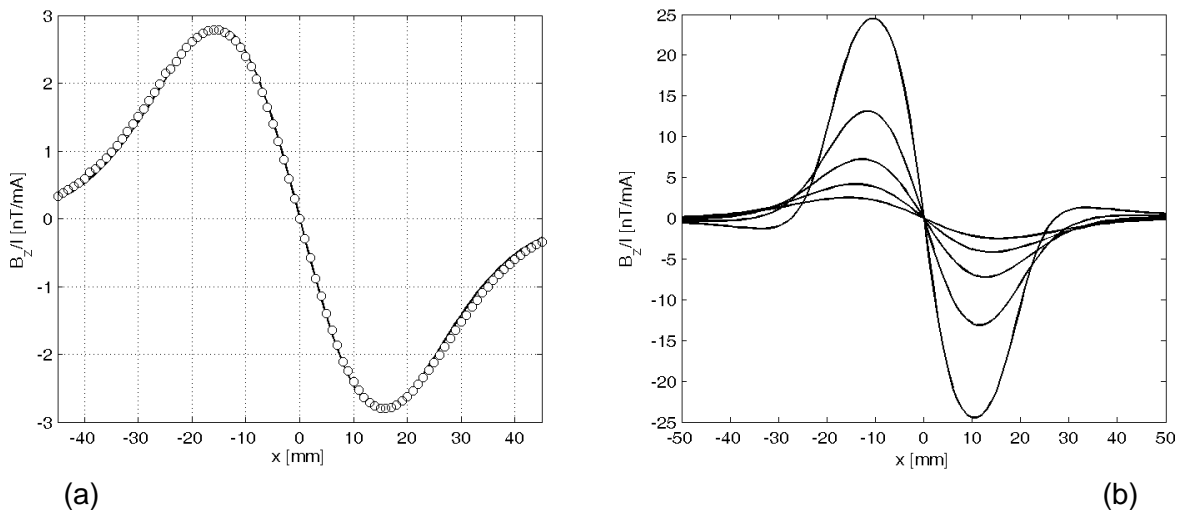


Fig.3 Coil in air. (a) Variation of  $B_z$  as a function of distance  $x$  across the excitation coil at a vertical distance of 28.9mm. Circles are measurements and straight lines represent theoretical calculations. (b) The same variation for five different distances from the coil ranging from  $z=10$ mm to 30mm in steps of 5mm.



### 3.2 Coil above an intact conductive plate

In this case also, when the SQUID is centered above the double-rectangle coil, the magnetic field measured is zero. Thus, again the SQUID was moved relative to the coil and the field profile is shown in Fig.4. Good agreement is observed between the experimental and theoretical results [13]. Both real and imaginary parts of the total magnetic field are shown.

The conductive plate in this case was Aluminum with conductivity  $\sigma=17\text{MS/m}$  and the distance between plate and coil (lift-off) was 2mm. The conductivity was measured by using the general purpose GE Phasec2D eddy current instrument that was equipped with a special conductivity probe.

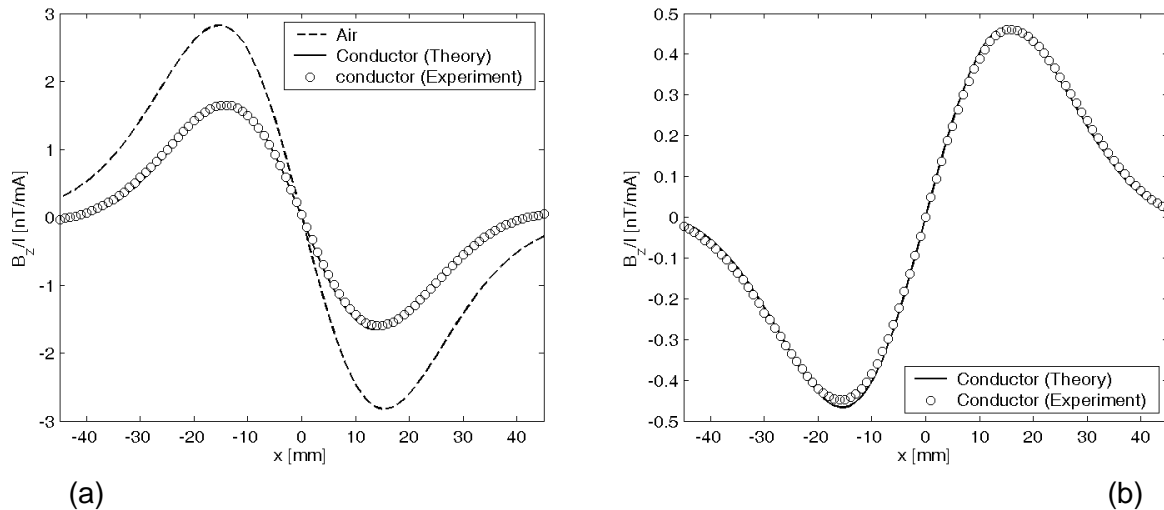


Fig.4 Coil in air and above conductive plate. Variation of  $B_z$  as a function of distance  $x$  across the excitation coil at a vertical distance of 28.9mm (a) Real part and (b) Imaginary part of total magnetic field. Circles are measurements and straight lines represent theoretical calculations. Note the decrease in the total magnetic field due to the conductive plate.

### 3.3 Coil above long through thickness slot

A long defect in the form of a through thickness slot was simulated by putting together two Aluminum (15mm thick) 0.120mm apart by means of a thin long insulating stripe. In this case, the coil was fixed at a distance 28.7mm below the SQUID. The coil's center was accurately positioned with respect to the SQUID so that the measured magnetic field is zero in air, i.e. before putting the plate. The coil and SQUID unit was then moved across the long slot, as shown in Fig.2b. The lift-off (coil to plate distance) in this case was 2.5mm. Measurements were taken at various frequencies, the experimental results shown in Fig.5 are for 3.225kHz. Fig.5 shows the comparison between experimental and theoretical results. The latter were derived using a semi-analytical method known as Truncated Region Eigenfunction Expansion (TREE) method that allows the solution of similar canonical problems in a rapid manner without sacrificing calculation accuracy [16-17].

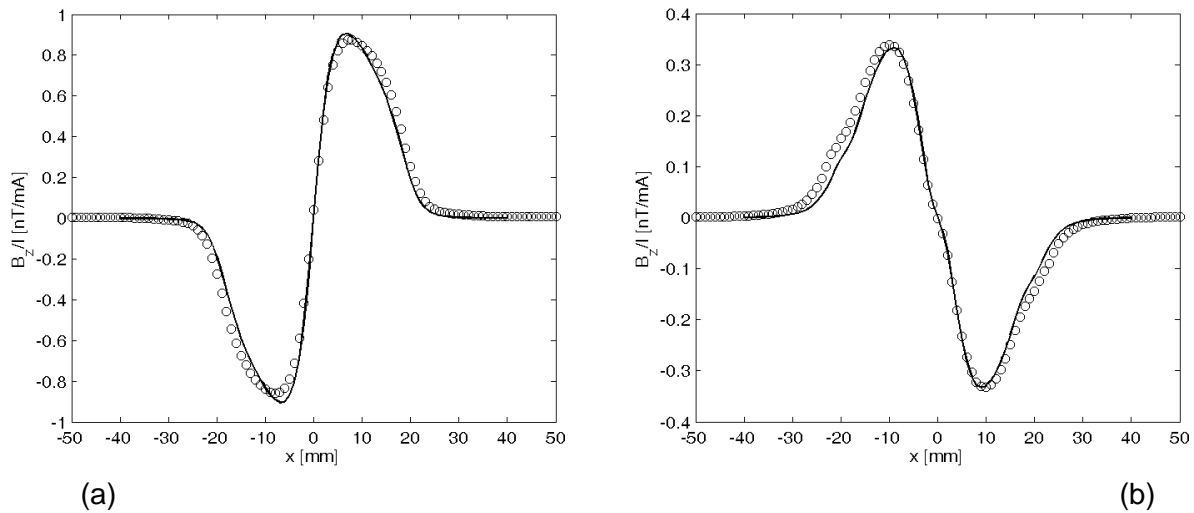


Fig.5 Coil and sensor above long through thickness slot in a plate conductor, variation of  $B_z$  as a function of  $x$ . (a) Real and (b) Imaginary part. Circles are measurements and straight lines represent theoretical calculations.

### 3.4 Coil above subsurface long slot

A similar measurement was taken for the case of a long slot at 10mm below surface, see Fig.6. This arrangement was achieved by adding an Aluminum plate of 10mm on the top of the configuration examined in the previous section 3.3. No theoretical results were available for this geometry.

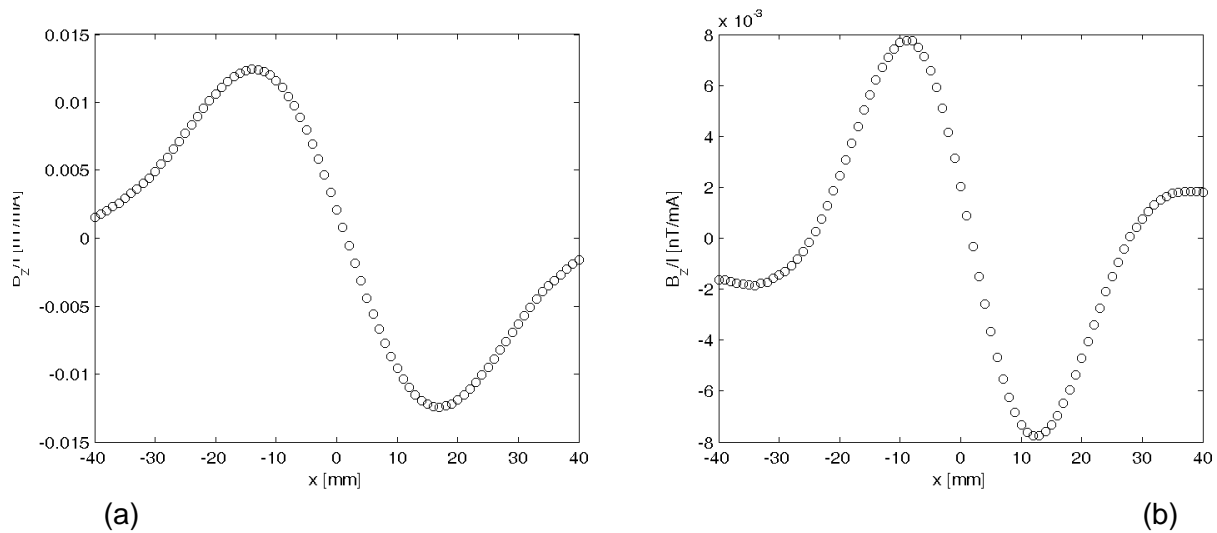


Fig.6 Coil and sensor above long subsurface slot in a plate conductor, variation of  $B_z$  as a function of  $x$ . (a) Real and (b) Imaginary part of experimental results.

A very low frequency of 120Hz was used in this case in order to achieve a sufficient penetration depth. Greater penetration can be achieved by using lower frequencies. In this case the defect signals become weaker and thus we have to increase the excitation current amplitude. This is actually the advantage of SQUID magnetometry when applied to eddy current inspections, that the excitation current can be



increased as the frequency decreases for sensing deep-lying defects. The only drawback is the simultaneous decrease in spatial resolution, which can be observed for example by comparing Fig.5 (surface slot signal) to Fig.6 (signal from same slot but subsurface). A more open and smooth signal is produced in the second case.

## 4 Conclusions and future work

Good agreement is observed between theoretical results and experimental measurements for a SQUID system measuring magnetic field for nondestructive applications. This shows the capability of SQUID in making accurate measurements even in an unshielded environment and also shows that modeling can be utilized for excitation coil optimization and evaluation of system performance. Future work is under way on similar quantitative measurements involving gradiometers, the simulations of alternative coil designs and flaw types. Finite length cracks will be modeled by utilizing numerical models involving integral methods and other semi-analytical models (we try to avoid time consuming FEM models).

## Acknowledgements

This work has been funded by the Ministry of National Education and Religious Affairs within the program “Archimedes II” for the promotion of technological research in Hellenic Technological Educational Institutes.

## References

- [1] Gallop J.C., *SQUIDS, the Josephson Effect and Superconducting Electronics*, Taylor & Francis, 1991.
- [2] Weinstock H. and Nisenoff M., *Non-destructive evaluation of metallic structures using a SQUID gradiometer*, SQUID '85, Proc. 3<sup>rd</sup> International Conference on Superconducting Quantum Devices, Hahlbohm H.D. and Lubbig H., Eds., 843--847, de Gruyter, Berlin, 1985; See also, *SQUID Sensors: Fundamentals, Fabrication and Application*, H. Weinstock (ed.), NATO ASI Series, Series E: Applied Sciences, 329, Kluwer, 1995.
- [3] Tavrin Y., Krause H.-J., Wolf W., Glyantsev V., Schubert J., Zander W., Bousack H., *Eddy current technique with high temperature SQUID for non-destructive evaluation of non-magnetic metallic structures*, *Cryogenics*, 36:83--86, 1996.
- [4] Kreuzbruck M.v., Allweins K., Ruhl T., Muck M., Heiden C., Krause H.-J., Hohmann R., *Defect detection and classification using a SQUID based multiple frequency eddy current NDE system*, *IEEE Transactions on Applied Superconductivity*, 11(1):1032--1037, 2001.
- [5] Claycomb J.R., Tralshawala N., Cho H.-M., Boyd M., Zou Z., *Simulation and design of a superconducting eddy current probe for nondestructive testing*, *Review of Scientific Instruments*, 69(2):499--506, 1998.
- [6] Claycomb J.R., Tralshawala N., Miller J.H., *Theoretical investigation of eddy-current induction for nondestructive evaluation by superconducting quantum interference devices*, *IEEE Transactions on Magnetics*, 36(1):292-298, 2000.
- [7] Morgan L.N.C., Carr C., Cochran A., McKirdy D.McA. and Donaldson G.B., *Electromagnetic non-destructive evaluation with simple HTS SQUIDS: Measurement and modelling*, *IEEE Transactions on Applied Superconductivity*, 5:3127--3130, 1995.
- [8] Ruosi A., Valentino M., Pepe G., Monebhurrun V., Lesselier D. and Duchene B., *High Tc SQUIDS and eddy-current NDE: a comprehensive investigation from real data to modelling*, *Meas. Sci. Technol.*, 11:1639--1648, 2000.
- [9] Pattabiraman M., Nagedran R. and Janawadkar M.P., *Rapid flaw depth estimation from SQUID-based eddy current nondestructive evaluation*, *NDT&E International*, 40:289--293, 2007.
- [10] Poulakis N., Theodoulidis T. and Liarokapis E., “SQUID magnetometer in eddy current non-destructive testing applications”, 5<sup>th</sup> NC NDT-HSNT, 2005.



- [11] Poulakis N. and Theodoulidis T., *The use of a SQUID for quantitative magnetic field measurements in the nanoTesla region for eddy current NDE*, Review of Progress in Quantitative Nondestructive Evaluation, Portland, 2006.
- [12] *pcSQUID™ User's Manual*, STAR Cryoelectronics, [www.starcryo.com](http://www.starcryo.com).
- [13] Theodoulidis T. and Kriezis E., *Impedance evaluation of rectangular coils for eddy current testing of planar media*, NDT&E International, 35:407--414, 2002.
- [14] Ditchburn R.J. and Burke S.K., *Planar rectangular spiral coils in eddy-current nondestructive inspection*, NDT&E International, 38:690--700, 2005.
- [15] Fava J.O. and Ruch M.C., *Calculation and simulation of impedance diagrams of planar rectangular spiral coils for eddy current testing*, NDT&E International, 39:414--424, 2006.
- [16] Bowler J.R. and Theodoulidis T., *Coil impedance variation due to induced current at the edge of a conductive plate*, Journal of Physics D: Applied Physics, 39:2862--2868, 2006.
- [17] Theodoulidis T. and Kriezis E., *Eddy current canonical problems (with applications to nondestructive evaluation)*, Techscience Press, 2006.